Revista Virtual de Química

Article

http://dx.doi.org/10.21577/1984-6835.20230005

Obtaining Mathematical Models Combined with Infrared Spectroscopy Data and the Use of *Artemia salina* as a Biological Indicator to Predict the Toxicity of the Biochars

Obtenção de Modelos Matemáticos Combinado com Espectroscopia de Infravermelho e o Uso de Artemia salina como Indicador Biológico para Predizer a Toxicidade de Biocarvões

Jeferson B. Eilert,[a,b] Flavia De Mello,[b] Estela M. C. C. Batista,[c] Jaqueline Nicolini,[b] Keller P. Nicolini[b]*

[a] Residente Técnico no Instituto Água e Terra, Rua Quintino Bocaiúva, Centro, CEP 84600-265, União da Vitória-PR, Brasil

[b] Instituto Federal de Educação, Ciência e Tecnologia do Paraná, Laboratório de Corantes e Processos Pirolíticos - LACOPPI, campus Palmas, CEP 85555-000, Palmas–PR, Brasil

[c] Universidade Federal do Paraná, Centro Politécnico, Jardim das Américas, CEP 81531-990, Curitiba-PR, Brasil

***E-mail:** estelamcc@gmail.com; jaqueline.nicolini@ifpr.edu.br; keller.nicolini@ifpr.edu.br

Recebido em: 28 de Julho de 2022

Aceito em: 18 de Outubro de 2022

Publicado online: 8 de Fevereiro de 2023

The simple analytical method described herein involves the use of infrared spectroscopy to analyze residues, consisting of biochar (C) and pyroligneous acid (PA), obtained from *Pinus*. The values for the concentration which is lethal to 50% of a sample of brine shrimp (*Artemia salina*) organisms (LC_{50}) were determined. For the chars produced at 400, 450 and 500 °C the LC_{50} values were > 5000 ppm. The LC_{50} value for PA is related to an increase in the intensity of the absorption bands of phenolic compounds at 1389 cm^{-1} and the C=C bands of aromatics at 1492 cm^{-1}. Pyrolysis temperatures of 250 and 300 °C are associated with the production of PA with $LC_{50} \geq 715$ ppm, accompanied by a lower intensity of the bands associated with the C-H of aromatic compounds (vibrational frequencies for C-H bending mode of benzene derivatives are observed from around 720 to 850 cm^{-1}). The biomodel results show that it is possible to predict the LC_{50} value through the application of mathematical models obtained from infrared spectroscopy data. The proposal explores the use of infrared spectroscopy combined with mathematical models (speed of analysis) and the use of *Artemia salina* as a biological indicator (low cost).

Keywords: Infrared spectroscopy; bioassays; mathematical models, biomass.

1. Introduction

The use of mathematical models is a promising strategy in different areas of application, used to predict the susceptibility of microorganisms to drugs, for example, has been shown to be important in several areas of medicine using different strategies.[1-3] Studies have shown that changes in the Fourier transform infrared spectra can be used to quantify lignin (ν C=C at 1514 cm^{-1}),[4] characterize the adsorption kinetics,[5] monitor chemical reactions,[6] monitor the production of stable aromatic rings,[7] and identify the functional groups.[8] The use of the absorption intensities of C=C in aromatics (close to 1640 cm^{-1}) and C-H in aliphatics (close to 2920 cm^{-1}) has been proposed to study stability index parameters.[9-12] The application of biological models is a useful strategy in ecotoxicology studies.[13, 14] Reports in the literature describe the use of infrared as a rapid analytical method to investigate, for example, biological activity in soil[15] and in a sealed container,[16] and to simulate the inhibition of the biological activity of benzoic acid derivatives.[17]

The brine shrimp (*Artemia salina*) is a small crustacean,[18] that was first used as a biological model in the area of nanoecotoxicology.[20] It has also been used to study the toxicity of oxides in saltwater ecosystems[21] and as a biomodel in other environmental toxicology assessments.[22] Tests based on crustaceans,[23] fish and algae require long exposure times and thus toxicity measurements based on microorganisms, which are more cost effective, are gaining popularity.[24] *Artemia salina* has been used as an experimental model to study the potential risks associated with biochars (derived from biomass) in ecosystems.[19]

Biomass is the matter originating from living organisms and thus includes trees, shrubs, herbaceous species, aquatic plants and algae, as well as animal residues and waste from agricultural harvesting and the processing of seeds or fruits.[25] Soft woods have ash contents of around 1% while the corresponding value for herbaceous biomass and agriculture residues is 15%.[25] One method for transforming biomass into energy is the thermochemical conversion process known as pyrolysis.[26] The conversion of the raw material into liquid fuel, which has

a higher energy density, facilitates transport and storage.[27] In general, the rapid pyrolysis of biomass results in different percentages of aromatic carbon and fixed carbon, respectively, according to the pyrolysis temperature as follows: 450 °C (21% and 37.5%), 500 °C (21% and 40.7%), 550 °C (25% and 42.2%), 600 °C (25% and 31.4%) and 732 °C (10% and 21.8%).[28,29] In the thermal decomposition of biomass, the formation of oxygenated gases, such as H_2O, CO and CO_2, starts at 150 °C and continues up to 300 °C. In the case of biomasses that have higher concentrations of alkaline metals and alkaline earth metals, such as Na, Mg, K and Ca, the formation of oxygenated gases starts at 200 °C, with a maximum peak at around 300 °C.[30] In the wood processing industry, in the south region of Paraná, *Pinus* is used as a feedstock and generates a large amount of waste. The aim of this study was to obtain mathematical models combined with infrared spectroscopy data and the use of *Artemia salina* as a biological indicator to predict the toxicity of the biochars (derived from *Pinus*) as an environmental potential plan, promoting sustainable development through an innovative approach in the context of the local wood processing industry.

2. Experimental

2.1. Pyrolysis

The mixture of residues from various *Pinus* species (mainly *Pinus taeda* and *Pinus elliottii*) employed in this study originated from tree trunks during wood processing. The material is a sample composed of approximately 25 kg of pine wood residues. The material was mixed, quartered, sized (particle size of less than 0.1 mm) and pyrolyzed at 6 different temperatures (250, 300, 350, 400, 450 and 500 ºC) to give 6 samples of the biochar (C) and 6 samples of the liquid product (pyroligneous acid, PA). Slow pyrolysis was carried out in an anaerobic reactor coupled to a Liebig condenser, with a heating ramp of 15 °C min^{-1}, at temperatures (ºC) of 250 (C_{250} and PA_{250}), 300 (C_{300} and PA_{300}), 350 (C_{350} and PA_{350}), 400 (C_{400} and PA_{400}), 450 (C_{450} and PA_{450}) and 500 °C (C_{500} and PA_{500}) for 3 h.[14,28,31]Each sample remained under heating (separately) for 3 h. Pyrolysis was carried out (separately) in triplicate. The pyrolyzed materials were then ground (≤ 150 µm) and homogenized. The gravimetric yields were determined for the different temperatures as percentage biochar mass (C), pyroligneous acid (PA) and ash content (AS).

2.2. Infrared (FTIR) spectroscopy and aromaticity index

Fourier transform infrared (FTIR) spectroscopy (Bio-Rad, USA) was carried out at the Laboratory of Automotive Fuels Analysis (*Laboratório de Análise de Combustíveis Automotivos* - LACAUT) on KBr plates. The samples were prepared by mixing 2 mg of each sample with 300 mg of anhydrous KBr (Neon, Brazil). The mixture was crushed in an 8-ton hydraulic press for the preparation of the pellets. The spectra for the samples were obtained within the range of 400 to 4000 cm^{-1}, with a scanning rate of 32 scans min^{-1}.

The aromaticity index[9-12] was calculated using the ratio $I_{C=C}/I_{C-H}$, where $I_{C=C}$ is the absorption intensity of the C=C of aromatics at 1640 cm^{-1} and I_{C-H} is the absorption intensity of the C-H of aliphatics at 2920 cm^{-1}.

2.3. Mathematical models, validation and statistical analysis

In order to evaluate the biological activity of the biochar and pyroligneous acid, mathematical models were developed with the aid of the BuildQSAR free software program (version 1.0.1.35).[32] The evaluation of the degree of prediction of the models was also carried out using the program BuildQSAR. Statistical validation and external validation were performed. A model with objects not included in it will give a high degree of predictability when the cross-validation correlation coefficient (Q^2) is close to 1 and standard deviation of cross-validation (S_{PRESS}) close to zero.[33] The models were generated from a semi-empirical method, considering the experimental investigation of the *in vitro* susceptibility - concentration is lethal to 50% of the organisms (LC_{50}) - of *Artemia salina* toward 6 samples of biochar and 6 samples of pyroligneous acid. The statistical analysis results were treated applying the Tukey test ($p < 0.05$).[34]

2.4. Lethal concentration (LC_{50})

Each biological activity test with *Artemia salina* lasted 48 h (i.e., 24 h for the egg eclosion, plus 24 h with the live organisms in contact with the amended medium). The eggs of *Artemia salina* were incubated in artificial seawater with 2% (SD ± 0.1) salinity, pH 8.5 (SD ± 0.5), at 27 °C (SD ± 3) for 24 h, being SD standard deviation. In the next step, the medium containing live *A. salina* organisms was amended as follows: a) each sample of $C_{250,}$ C_{300}, C_{350}, C_{400}, C_{450} and C_{500} was tested at concentrations of 0, 1,000, 5,000, 10,000 and 50,000 ppm; and b) each sample of $PA_{250,}$ PA_{300}, PA_{350}, PA_{400}, PA_{450} and PA_{500} was tested at concentrations of 0, 100, 200, 417, 625 and 1,250 ppm. The counting of the dead organisms was carried out after 24 h to calculate the numbers in the amended aqueous media and determine which concentration is lethal to 50% of the organisms (LC_{50}). The tests were carried out with 10 replicates (10 to 12 individuals per replicate). The percent of dead larvae was calculated based on the number of live individuals at the initial time (24 h) in relation to the number after 24 h in the amended environment,[35] using Equation 1.

$$\%D = \left[\frac{(N - B - C)}{N - C}\right] \times 100 \qquad (1)$$

where: %D is the percentage of the dead larvae in each sample, N is the average number of larvae before starting the test, B is the average number of dead larvae in each sample and C is the average number of dead larvae in the control samples. The data obtained were converted into percentages based on the relation between the percentage mortality and the sample concentration. The lethal concentration (LC_{50}) was determined from the linear correlation coefficient.

3. Results and Discussion

It can be observed from the infrared spectra (Figure 1) for C_{250}, C_{300}, C_{350}, C_{400}, C_{450} and C_{500} that the intensity of the bands at 3448 cm^{-1} (corresponding to the O-H of hemicellulose and lignin), 2920 cm^{-1} (associated with the C-H of alkyl, aliphatic and aromatic groups),[36] 1736 cm^{-1} (corresponding to C=O), 1709 cm^{-1} (associated with the C-H of alkly, aliphatic and aromatic groups) and 1622 cm^{-1} (related to the C=O of aromatic groups) are lower for the C_{400}, C_{450} and C_{500} samples, which have the highest LC_{50} values (Table 1). After the heating of the material, the aromatic structures, which are more stable than aliphatic structures, show greater resistance to degradation and volatilization and thus they are present in higher concentrations in the biochar samples obtained at higher temperatures. Figure 1 shows that the intensity of the band at 667 cm^{-1} (C-C of aromatics) increases with an increase in the pyrolysis temperature. The intensities of the absorption bands at 622 and 667 cm^{-1} (C-C of aromatics)[36] and 3268 cm^{-1} are directly proportional to the LC_{50} while the band at 2949 cm^{-1} (C-H of hydrocarbon)[37] (Figure 1) is inversely proportional to the biological activity (Table 1).

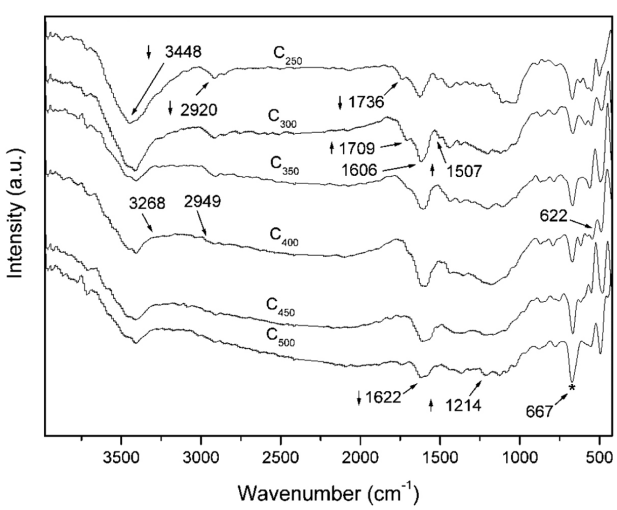

Figure 1. Infrared spectra for biochar samples obtained from pyrolysis of *Pinus* spp. at 250, 300, 350, 400, 450 and 500 °C

The lethal concentration, aromaticity index and absorption intensities at 3448 cm^{-1} (O-H), 2920 cm^{-1} (C-H), 1622 cm^{-1} (C=O) and 667 cm^{-1} (C=C) (Figure 1 and Table 1) showed that, for the biochars, higher LC_{50} values are associated with higher aromaticity indexes, higher intensity at 667 cm^{-1}, lower intensities at 3448, 2920 and 1622 cm^{-1} and pyrolysis temperatures of 400, 450 and 500 °C.

The reduction in the intensity at around 3440 cm^{-1} (Figure 1) with an increase in the pyrolysis temperature (250→500 °C) suggests the removal of hydroxyl groups from the cellulose.[38] In a similar study, Park *et al*. (2018) reported the generation of pyroligneous acid, containing phenol, 2-methoxy, phenol, 2,6-dimethoxy, E-11-hexadecanoic acid and ethyl ester as the major components,[39] and biochar with a high content of condensed aromatic structures.[40, 41]

At the pyrolysis temperatures (Figure 1) of 250, 300, 350, 400, 450 and 500 °C the C-C stretching (622 cm^{-1}) bonds are maintained, increasing the gravimetric biochar yield. The results for the biochar samples obtained from pyrolysis at 250, 300, 350, 400, 450 and 500 °C show that the higher the pyrolysis temperature the higher the aromaticity index and LC_{50} will be. The results for the pyroligneous acid obtained at pyrolysis temperatures of 250, 300, 350, 400, 450 and 500 °C indicate that increasing the pyrolysis temperature leads to a higher aromaticity index and greater toxicity (Table 1).

In the case of PA, the samples generated at 250 °C showed the highest LC_{50} values and thus had the lowest toxicity toward *Artemia salina*, while for the biochar samples (C), those produced at temperatures ≥ 400 °C had the highest lethal concentrations, as shown in Table 1.

Based on the linear correlation coefficient, the lethal concentration (LC_{50}) was determined and Table S1 shows the percentage mortality values for each temperature. The biochar samples obtained at 400, 450 and 500 °C show the lowest toxicity and all samples of pyroligneous acid with concentrations above 417 ppm showed lethality of 100% (Table S1).

Figure 2 shows the infrared spectra for the samples PA_{250}, PA_{300}, PA_{350}, PA_{400}, PA_{450} and PA_{500}, where the appearance of bands is directly proportional to the pyrolysis temperature: at 2900 cm^{-1}, corresponding to the C-H of alkyl, aliphatic and aromatic groups;[36] at 1507 cm^{-1}, related to the C=O of ketone and carbonyl groups,[36] and at 1200 cm^{-1}, associated with the C-O of alcohols, esters, carboxylic acid and ethers as well as phenolic compounds. The presence of the band at 1000 cm^{-1} related to C-O and C-H groups is inversely proportional to the pyrolysis temperature. Studies using infrared spectra are versatile and this technique speeds up the monitoring process.

For the PA samples, an increase in the LC_{50} value is also associated with a reduction in the intensity of the absorption band at 727 cm^{-1} (C-H of aromatics, vibrational frequencies for C-H bending mode of benzene derivatives)[36] and increases in the intensity of the absorption bands at 1389 cm^{-1} (phenolic compounds) and 1492 cm^{-1} (C=C of aromatics)[36], as shown in Figure 2. The presence of aromatic compounds alters the metabolism of carbohydrates[42] and proteins[43], these being metabolized by bacteria and converted into CO_2.[44]

Table 1. Aromaticity index and toxicity toward *Artemia salina* and pyrolysis temperature used to obtain biochar (C) and pyroligneous acid (PA)

Samples	$I_{C=C}/I_{C-H}$	LC_{50} (ppm)	$\left(\log\frac{1}{LC_{50}}\right)$ (ppm)
		Biochar	
C_{250}	1.164	18438	-4.266
C_{300}	1.135	5171	-3.714
C_{350}	1.130	7845	-3.894
C_{400}	1.150	≥50000	-4.699
C_{450}	1.174	≥50000	-4.699
C_{500}	1.173	≥50000	-4.699
		Pyroligneous acid	
PA_{250}	0.277	733	-2.865
PA_{300}	0.268	715	-2.854
PA_{350}	0.296	518	-2.714
PA_{400}	0.308	607	-2.783
PA_{450}	0.339	512	-2.709
PA_{500}	0.335	645	-2.810

$I_{C=C}$: absorption intensity of the C=C of aromatics at 1640 cm^{-1}. I_{C-H}: absorption intensity of the C-H of aliphatics at 2920 cm^{-1}. $I_{C=C}/I_{C-H}$: aromaticity index.[9-12] LC_{50}: toxicity toward *Artemia salina*. $\left(\log\frac{1}{LC_{50}}\right)$: base 10 logarithm of toxicity toward *Artemia salina*

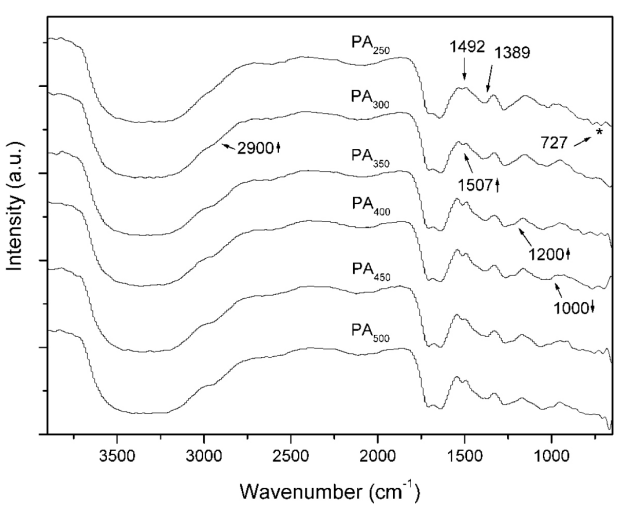

Figure 2. Infrared spectra for samples of pyroligneous acid obtained from *Pinus* spp. pyrolyzed at 250, 300, 350, 400, 450 and 500 °C

After the gravimetric analysis of the pyrolyzed material (Figure S1) it was observed that the sample obtained at 400 °C shows a biochar (C) yield of 35.4% (± 1.6) and a pyroligneous acid (PA) yield of 38.9% (± 1.6). Figure S1 shows that the gravimetric yields of biochar and pyroligneous acid are equivalent (37.0%) at a temperature of 385 °C (intercept). In general, the ash content is inversely proportional to the gravimetric biochar yield.

Based on the intensities of the bands on the infrared spectra we obtained Equation 2, to predict the biological activity $\left(\log\frac{1}{LC_{50}}\right)$ of the biochar samples through a linear model with $R^2 = 0.956$ and $Q^2 = 0.860$. The *I* parameter corresponds to the intensity of the absorption unit, at 667 cm^{-1}, R^2 represents the correlation coefficient of the equation and Q^2 is related to the prediction capacity of Equation 2.

$$\log\frac{1}{LC_{50}} = 0.22429I_{[667]} - 20.97423 \quad (2)$$

Also, based on the intensities of the bands on the infrared spectra at 727 cm^{-1}, Equation 3 is proposed, to predict the biological activity $\left(\log\frac{1}{LC_{50}}\right)$ of the pyroligneous acid samples through a linear model with $R^2 = 0.972$ and $Q^2 = 0.923$.

$$\log\frac{1}{LC_{50}} = 0.03673I_{[727]} - 2.84998 \quad (3)$$

An evaluation of the degree of predictability of the model calculated using the BuildQSAR software program (version 1.0.1.35)[32] indicated that there is a high degree of predictability when the cross-validation correlation coefficient (Q^2) is close to 1 and S_{PRESS} close to zero,[33] as calculated from Equations 2 and 3 (Table S2). Equations 2 and 3 were validated by statistical validation based on R^2, s, F, Q^2 and S_{PRESS} (Table S2). The parameter s is the standard deviation, S_{PRESS} is the standard deviation of cross-validation, and F is the ratio between the variability explained by the model and the variability that remains unexplained. The

equations were also validated using external validation,[45] where the value of $\left(\log\frac{1}{LC_{50}}\right)_{Observed}$ is close to the value of $\left(\log\frac{1}{LC_{50}}\right)_{Predicted}$ (Table S2). Equations 2 and 3 show good degrees of predictability of the toxicity of samples of biochar (C) and pyroligneous acid (PA) derived from *Pinus* sp. obtained by pyrolysis in a reducing atmosphere at 250 - 500 °C.

Studies have demonstrated that pyroligneous acid is effective as a fungicide, due to the presence of phenolic compounds,[46] and as an insecticide, due to the presence of hexadecanoic acid and fatty acids derived from octadecanoic acid.[47] In this study, the highest aromaticity indexes for C and PA (Table 1) were obtained at 450 °C, which is consistent with reports in the literature.[28, 48-50] The pyrolysis temperature of 450 °C is associated with the lowest LC_{50} for PA (higher toxicity) and one of the highest LC_{50} values for C (lower toxicity), as shown in Table 1.

A decrease in the toxicity of the biochars (higher LC_{50} value) is also associated with an increase in band intensity in the region of 667 cm^{-1}, which is attributed to the C-H of mono-substituted aromatics[36] from of lignin degradation. Studies demonstrate that hemicellulose is reactive at 160-360 °C, cellulose decomposes at 240-390 °C and lignin undergoes degradation at 200-850 °C.[29] Based on this finding, it is proposed that biochars produced through slow pyrolysis above 400 °C would show lower toxicity toward *Artemia salina*.

The proposed procedure does not generate hazardous waste, highlighting the environmental potential of this strategy, promoting sustainable development through an innovative approach. Infrared is a spectroscopic technique that has been previously applied for the investigation of the biological activity of natural products.[53] In this study, the determination of biological activity is approached in two ways: a) experimentally: using *Artemia salina* applying a classic and low cost method with an average analysis time of 48 h; and b) theoretically: using infrared spectroscopy combined with mathematical models. This approach brings as a novelty a rapid analysis strategy (around 30 min) that is able to predict the biological activity, with results of around 86.0% ($Q^2 = 0.860$) and 92.3% ($Q^2 = 0.923$), for C and PA, respectively.

4. Conclusions

The biochar with the highest toxicity toward *Artemia salina* was the sample produced at 300 °C and biochars produced at 400, 450 and 500 °C showed the lowest toxicities. In the case of pyroligneous acid, the highest toxicity toward *Artemia salina* was observed for the sample generated at 450 °C while the sample generated at 250 °C showed the lowest toxicity. Thus, the biochars generated at higher temperatures have lower toxicity and they generate pyroligneous acid with higher toxicity toward *Artemia salina*. Biochars produced by slow pyrolysis at 400, 450 and 500 °C have $LC_{50} > 5000$ ppm. Based on the biomodel results of this study, the biological activity of *Pinus* spp. biochars and pyroligneous acid was correlated mathematically with the infrared spectroscopy data, applying simple and safe procedures.

Supplementary Data

Table S1. Sample lethality (%) as a function of concentration (ppm). Table S2. QSARs Validation. Figure S1. Relation between gravimetric biochar (C) yield, pyroligneous acid (PA) yield and ash content (AS), obtained for samples of *Pinus* spp. biomass subjected to pyrolysis at 250, 300, 350, 400, 450 and 500 °C. Supplementary data associated with this article can be found free of charge in the online version at https://rvq.sbq.org.br/.

Acknowledgments

The authors are grateful to SBQ and the editors of the RVq by the invitation, to the Programa Institucional de Apoio à Iniciação Científica da Fundação Araucária (PIBIC-FA), Programa Institucional de Bolsas de Incentivo à Inovação do Instituto Federal do Paraná (PIBIN/IFPR), Laboratório de Análises de Combustíveis Automotivos (LACAUT) and Laboratório de Corantes e Processos Pirolíticos (LACOPPI).

References

1. Dowdy, D. W.; Chaisson, R. E.; Maartens, G.; Corbett, E. L.; Dorman, S. E.; Impact of enhanced tuberculosis diagnosis in South Africa: a mathematical model of expanded culture and drug susceptibility testing. *Proceedings of the National Academy of Sciences* **2008**, *105*, 11293. [Crossref] [PubMed]
2. Machado, C.; Nicolini, K. P.; Nicolini, J.; Estudo de QSAR para SARS-CoV-2. *Química Nova* **2020**, *43*, 1258. [Crossref]
3. Granich, R. M.; Gilks, C. F.; Dye, C.; De Cock, K. M.; Williams, B. G.; Universal voluntary HIV testing with immediate antiretroviral therapy as a strategy for elimination of HIV transmission: a mathematical model. *The Lancet* **2009**, *373*, 48. [Crossref] [PubMed]
4. Bui, N. Q.; Fongarland, P.; Rataboul, F.; Dartiguelongue, C.; Charon, N.; Vallée, C.; Essayem, N.; FTIR as a simple tool to quantify unconverted lignin from chars in biomass liquefaction process: Application to SC ethanol liquefaction of pine wood. *Fuel Processing Technology* **2015**, *134*, 378. [Crossref]
5. Reynel-Avila, H. E.; Mendoza-Castillo, D. I.; Bonilla-Petriciolet, A.; Relevance of anionic dye properties on water decolorization performance using bone char: Adsorption kinetics, isotherms and breakthrough curves. *Journal of Molecular Liquids* **2016**, *219*, 425. [Crossref]

6. Peng, C.; Zhai, Y.; Zhu, Y.; Xu, B.; Wang, T.; Li, C.; Zeng, G.; Production of char from sewage sludge employing hydrothermal carbonization: Char properties, combustion behavior and thermal characteristics. *Fuel* **2016**, *176*, 110. [Crossref]
7. Zhao, Y.; Feng, D.; Zhang, Y.; Huang, Y.; Sun, S.; Effect of pyrolysis temperature on char structure and chemical speciation of alkali and alkaline earth metallic species in biochar. *Fuel Processing Technology* **2016**, *141, Part 1*, 54. [Crossref]
8. Hu, J.; Shen, D.; Wu, S.; Zhang, H.; Xiao, R.; Effect of temperature on structure evolution in char from hydrothermal degradation of lignin. *Journal of Analytical and Applied Pyrolysis* **2014**, *106*, 118. [Crossref]
9. Huang, G. F.; Wu, Q. T.; Wong, J. W. C.; Nagar, B. B.; Transformation of organic matter during co-composting of pig manure with sawdust. *Bioresource Technology* **2006**, *97*, 1834. [Crossref] [PubMed]
10. Hsu, J.-H.; Lo, S.-L.; Chemical and spectroscopic analysis of organic matter transformations during composting of pig manure. *Environmental Pollution* **1999**, *104*, 189. [Crossref]
11. Chefetz, B.; Hatcher, P. G.; Hadar, Y.; Chen, Y.; Chemical and Biological Characterization of Organic Matter during Composting of Municipal Solid Waste. *Journal of Environmental Quality* **1996**, *25*, 776. [Crossref]
12. Dick, D. P.; Santos, J. H. Z.; Ferranti, E. M.; Chemical characterization and infrared spectroscopy of soil organic matter from two Southern Brazilian soils. *Revista Brasileira de Ciência do Solo* **2003**, *27*, 29. [Crossref]
13. Girelli, G. C.; Cordeiro, M. E.; Nicolini, J.; Nicolini, K. P.; Reflectance and ultraviolet spectroscopy: predicting the relative growth of *Saccharomyces cerevisiae* in *Pine* biomass. *Spectroscopy Letters* **2019**, *52*, 1. [Crossref]
14. Guimarães, A. R.; Cordeiro, M. E.; Nicolini, J.; Nicolini, K. P.; Use of ultrasound to modify the pyrolyzed biomass of *Pinus* spp. and the implications for biological models. *Information Processing in Agriculture* **2018**, *5*, 199. [Crossref]
15. Reeves, J. B.; McCarty, G. W.; Meisinger, J. J.; Near Infrared Reflectance Spectroscopy for the Determination of Biological Activity in Agricultural Soils. *Journal of Near Infrared Spectroscopy* **2000**, *8*, 161. [Link]
16. Sussman, M. L.; Ahnell, J. E.; McCarthy, L. R.; Detection of the presence of biological activity in a sealed container utilizing infrared analysis of carbon dioxide and apparatus therefor. *Google Patents:* **1992**. [Link]
17. Xavier, T. S.; Joe, I. H.; FT-IR, Raman and DFT study of 2-amino-5-fluorobenzoic acid and its biological activity with other halogen (Cl, Br) substitution. *Spectrochimica Acta Part A: Molecular and Biomolecular Spectroscopy* **2011**, *79*, 332. [Crossref] [PubMed]
18. Giwa, A.; Dufour, V.; Al Marzooqi, F.; Al Kaabi, M.; Hasan, S. W.; Brine management methods: Recent innovations and current status. *Desalination* **2017**, *407*, 1. [Crossref]
19. Zhu, S.; Luo, F.; Chen, W.; Zhu, B.; Wang, G.; Toxicity evaluation of graphene oxide on cysts and three larval stages of *Artemia salina*. *Science of The Total Environment* **2017**, *595*, 101. [Crossref] [PubMed]
20. Libralato, G.; The case of *Artemia* spp. in nanoecotoxicology. *Marine Environmental Research* **2014**, *101*, 38. [Crossref] [PubMed]
21. Sarkheil, M.; Johari, S. A.; An, H. J.; Asghari, S.; Park, H. S.; Sohn, E. K.; Yu, I. J.; Acute toxicity, uptake, and elimination of zinc oxide nanoparticles (ZnO NPs) using saltwater microcrustacean, *Artemia franciscana*. *Environmental Toxicology and Pharmacology* **2018**, *57*, 181. [Crossref] [PubMed]
22. Lavtizar, V.; Kimura, D.; Asaoka, S.; Okamura, H.; The influence of seawater properties on toxicity of copper pyrithione and its degradation product to brine shrimp *Artemia salina*. *Ecotoxicology and Environmental Safety* **2018**, *147*, 132. [Crossref] [PubMed]
23. Bustos-Obregon, E.; Vargas, Á., Chronic toxicity bioassay with populations of the crustacean Artemia salina exposed to the organophosphate diazinon. *Biological Research* **2010**, *43*, 357. [Crossref] [PubMed]
24. Parvez, S.; Venkataraman, C.; Mukherji, S.; A review on advantages of implementing luminescence inhibition test (*Vibrio fischeri*) for acute toxicity prediction of chemicals. *Environment International* **2006**, *32*, 265. [Crossref] [PubMed]
25. Yaman, S.; Pyrolysis of biomass to produce fuels and chemical feedstocks. *Energy Conversion and Management* **2004**, *45*, 651. [Crossref]
26. Raveendran, K.; Ganesh, A.; Khilar, K. C.; Pyrolysis characteristics of biomass and biomass components. *Fuel* **1996**, *75*, 987. [Crossref]
27. Van de Velden, M.; Baeyens, J.; Brems, A.; Janssens, B.; Dewil, R.; Fundamentals, kinetics and endothermicity of the biomass pyrolysis reaction. *Renewable Energy* **2010**, *35*, 232. [Crossref]
28. Brewer, C.; Unger, R.; Schmidt-Rohr, K.; Brown, R.; Criteria to select biochars for field studies based on biochar chemical properties. *BioEnergy Research* **2011**, *4*, 312. [Crossref]
29. Vamvuka, D.; Kakaras, E.; Kastanaki, E.; Grammelis, P.; Pyrolysis characteristics and kinetics of biomass residuals mixtures with lignite. *Fuel* **2003**, *82*, 1949. [Crossref]
30. Sonobe, T.; Worasuwannarak, N.; Kinetic analyses of biomass pyrolysis using the distributed activation energy model. *Fuel* **2008**, *87*, 414. [Crossref]
31. Nicolini, K. P.; Casagrande, M.; De Jesus, A. C.; *Pirólise de Biomassa em Baixas Temperaturas*, 1ª. ed., Átomo: Campinas, 2013. [Link]
32. De Oliveira, D. B.; Gaudio, A. C.; BuildQSAR: a new computer program for QSAR analysis. *Quantitative Structure-Activity Relationships: An International Journal Devoted to Fundamental and Practical Aspects of Electroanalysis* **2000**, *19*, 599. [Crossref] [PubMed]
33. Gaudio, A. C.; Zandonade, E.; Proposição, validação e análise dos modelos que correlacionam estrutura química e atividade biológica. *Química Nova* **2001**, *24*, 658. [Crossref]
34. CCA - Centro de Ciências Agrárias - Teste de Tukey. Disponível em: <https://www.cca.ufscar.br/pt-br/servicos/teste-de-tukey>. Acesso em: 13 julho 2022.
35. Stefanello, M. É. A.; Salvador, M. J.; Ito, I. Y.; Macari, P. A. T.; Avaliação da atividade antimicrobiana e citotóxica de extratos de *Gochnatia polymorpha* ssp. *floccosa*. *Revista Brasileira de Farmacognosia* **2006**, *16*, 525. [Crossref]

36. Yang, H.; Yan, R.; Chen, H.; Lee, D. H.; Zheng, C.; Characteristics of hemicellulose, cellulose and lignin pyrolysis. *Fuel* **2007**, *86*, 1781. [Crossref]
37. Souza, B.; Moreira, A.; Teixeira, A.; TG-FTIR coupling to monitor the pyrolysis products from agricultural residues. *Journal of Thermal Analysis and Calorimetry* **2009**, *97*, 637. [Crossref]
38. Czaderna, A.; Kocemba, A.; Kozanecki, M.; Mucha, M.; Mróz, P.; The influence of cellulose derivatives on water structure in gypsum. *Construction and Building Materials* **2018**, *160*, 628. [Crossref]
39. Park, J.; Riaz, A.; Insyani, R.; Kim, J.; Understanding the relationship between the structure and depolymerization behavior of lignin. *Fuel* **2018**, *217*, 202. [Crossref]
40. Zhang, L.; Hu, S.; Xu, K.; Jiang, L.; Wang, Y.; Su, S.; Xiao, Y.; Shan, L.; Shen, W.; Li, H.; Chen, G.; Xiang, J.; Study on the structural evolution of semi-chars and their solvent extracted materials during pyrolysis process of a Chinese low-rank coal. *Fuel* **2018**, *214*, 363. [Crossref]
41. Wiedemeier, D. B.; Abiven, S.; Hockaday, W. C.; Keiluweit, M.; Kleber, M.; Masiello, C. A.; McBeath, A. V.; Nico, P. S.; Pyle, L. A.; Schneider, M. P. W.; Smernik, R. J.; Wiesenberg, G. L. B.; Schmidt, M. W. I.; Aromaticity and degree of aromatic condensation of char. *Organic Geochemistry* **2015**, *78*, 135. [Crossref]
42. Patel, J. G.; Kumar, J. N.; Khan, S. R.; Consequences of environmentally hazardous polycyclic aromatic hydrocarbon-anthracene treatment on cyanobacteria. *International Journal of Applied Sciences and Biotechnology* **2015**, *3*, 381. [Crossref]
43. Marqués, S.; Holtel, A.; Timmis, K. N.; Ramos, J.; Transcriptional induction kinetics from the promoters of the catabolic pathways of TOL plasmid pWW0 of *Pseudomonas putida* for metabolism of aromatics. *Journal of Bacteriology* **1994**, *176*, 2517. [Crossref] [PubMed]
44. Butler, J. E.; He, Q.; Nevin, K. P.; He, Z.; Zhou, J.; Lovley, D. R.; Genomic and microarray analysis of aromatics degradation in *Geobacter metallireducens* and comparison to a *Geobacter* isolate from a contaminated field site. *BMC Genomics* **2007**, *8*, 180. [Crossref] [PubMed]
45. Alves, V. M.; Braga, R. C.; Muratov, E. N.; Andrade, C. H.; Quimioinformática: Uma Introdução. *Química Nova* **2018**, *41*, 202. [Crossref]
46. Tiilikkala, K.; Fagernäs, L.; Tiilikkala, J.; History and use of wood pyrolysis liquids as biocide and plant protection product. *The Open Agriculture Journal* **2010**, *13*, 111. [Crossref]
47. Suqi, L.; Caceres, L.; Schieck, K.; Booker, C. J.; McGarvey, B. M.; Yeung, K. K.-C.; Pariente, S.; Briens, C.; Berruti, F.; Scott, I. M.; Insecticidal Activity of Bio-oil from the Pyrolysis of Straw from *Brassica* spp. *Journal of agricultural and food chemistry* **2014**, *62*, 3610. [Crossref] [PubMed]
48. Martins, A. F.; Diniz, J.; Stahl, J. A.; Cardoso, A. D. L.; Caracterização dos produtos líquidos e do carvão da pirólise de serragem de eucalipto. *Química Nova* **2007**, *30*, 873. [Crossref]
49. Lu, R.; Sheng, G.-P.; Hu, Y.-Y.; Zheng, P.; Jiang, H.; Tang, Y.; Yu, H.-Q.; Fractional characterization of a bio-oil derived from rice husk. *Biomass and Bioenergy* **2011**, *35*, 671. [Crossref]
50. Li, J.; Wu, L.; Yang, Z.; Analysis and upgrading of bio-petroleum from biomass by direct deoxy-liquefaction. *Journal of Analytical and Applied Pyrolysis* **2008**, *81*, 199. [Crossref]
51. Browne, R. A.; Davis, L. E.; Sallee, S. E.; Effects of temperature and relative fitness of sexual and asexual brine shrimp *Artemia*. *Journal of Experimental Marine Biology and Ecology* **1988**, *124*, 1. [Crossref]
52. Busa, W. B.; Crowe, J. H.; Intracellular pH regulates transitions between dormancy and development of brine shrimp (*Artemia salina*) embryos. *Science* **1983**, *221*, 366. [Crossref] [PubMed]
53. Srivastava, A. K.; Pandey, A. K.; Jain, S.; Misra, N.; FT-IR spectroscopy, intra-molecular C–H···O interactions, HOMO, LUMO, MESP analysis and biological activity of two natural products, triclisine and rufescine: DFT and QTAIM approaches. *Spectrochimica Acta Part A: Molecular and Biomolecular Spectroscopy* **2015**, *136*, 682. [Crossref] [PubMed]